Identification of Necroptosis-Related Long Noncoding RNAs for Immunotherapy Selection and Prognosis Prediction in Patients with Colorectal Cancer

Zhihua Chen
The First Affiliated Hospital of Fujian Medical University
Yilin Lin
Peking University
Suyong Lin
The First Affiliated Hospital of Fujian Medical University
Xiaoyu Yang
Fujian Medical University
Shao-Qin Chen (chenshaoqin1613@163.com)
The First Affiliated Hospital of Fujian Medical University

Article

Keywords: Long Noncoding RNA, Necroptosis, Immunotherapy, Prognosis, Colorectal Cancer

Posted Date: May 18th, 2022

DOI: https://doi.org/10.21203/rs.3.rs-1602827/v1

Identification of Necroptosis-Related Long Noncoding RNAs for Immunotherapy Selection and Prognosis Prediction in Patients with Colorectal Cancer.

Zhihua Chen[a], Yilin Lin[b], Suyong Lin[a], Xiaoyu Yang[c], Shaoqin Chen[a];

Corresponding author: Shao-Qin Chen, Email:chenshaoqin1613@163.com.

Co-Corresponding author: Xiaoyu Yang, Email:yxyfj@163.com

The first author:Zhihua Chen, Email: chenzhihua139@126com.

Co-first author: Yilin Lin, Email: linyilin0430@163.com.

The third author: Suyong Lin,Email:641590501@qq.com

a Department of Gastrointestinal Surgery, The First Affiliated Hospital of Fujian Medical University,Fuzhou 350004,China.

b Peking University Health Science Center

c School of Basic Medicine Sciences, Fujian Medical University,Fuzhou 350004,China.

Corresponding author: Shao Qin Chen,

Correspondence to: Department of Gastrointestinal Surgery, The First Affiliated Hospital of Fujian Medical University,Fuzhou 350004,China;Tel:+86 13615045151,Fax:+86 059187982082,

Email: chenshaoqin1613@163.com.

Abstract

Background: Tumor recurrence and metastasis lead to a poor prognosis in colorectal cancer (CRC). Necroptosis is closely related to the tumor microenvironment (TME) and affects tumor recurrence and metastasis. We aimed to stratify CRC patients according to necroptosis-related long noncoding RNAs (lncRNAs), which can be used to not only evaluate prognosis and improve precision medicine in clinical practice but also evaluate the efficacy of immunotherapy and guide the selection of immunotherapeutic methods.

Methods: A lncRNA expression profile was collected from The Cancer Genome Atlas (TCGA). Necroptosis-related lncRNAs were identified by coexpression analysis. Cox regression analysis identified a necroptosis-related lncRNA signature. Then, the value of this signature was comprehensively and multidimensionally evaluated, and its fidelity was assessed with clinical CRC data and compared with that of six other

lncRNA signatures for CRC prognosis prediction. Gene set enrichment analysis (GSEA), TME analysis and prediction of the half-maximal inhibitory concentration (IC50) were also performed according to the risk score (RS) of the signature.

Results: An 8-lncRNA signature significantly associated with overall survival (OS) was constructed, and its fidelity was validated with clinical CRC data. Most of the areas under the receiver operating characteristic (ROC) curve (AUCs) for 1-, 3- and 5-year OS for this signature were higher than those for the other six lncRNA signatures. OS, disease-specific survival (DSS) and the progression-free interval (PFI) were all significantly poorer in the high-risk group. The RS of the signature showed good concordance with the predicted prognosis, with AUCs for 1-, 3- and 5-year OS of 0.79, 0.81 and 0.77, respectively. Additionally, the calibration plots for this signature combined with clinical factors could effectively improve the ability to predict OS. The RS was correlated with tumor stage, lymph node metastasis and distant metastasis. Most of the enriched Kyoto Encyclopedia of Genes and Genomes (KEGG) and Gene Ontology (GO) terms were tumor metastasis-related pathways in the high-risk group, which showed greater infiltration of immunosuppressive cells, such as cancer-associated fibroblasts (CAFs), hematopoietic stem cells and M2 macrophages, but fewer infiltrating antitumor effector immune cells, such as CD8+ T cells and regulatory T cells (Tregs). We explored additional potential immune checkpoint genes and immunotherapeutic and chemotherapeutic drugs with relatively low IC50 values.

Conclusions: We identified a signature with strong fidelity that could stably predict prognosis and might be implicated in the TME and metastasis of CRC. Furthermore, additional potential immune checkpoint genes and immunotherapeutic and chemotherapeutic drugs were explored.

Key words: Long Noncoding RNA, Necroptosis, Immunotherapy, Prognosis, Colorectal Cancer

Introduction

Despite significant reductions in the incidence and mortality of colorectal cancer (CRC) over several decades, CRC[1] is the third most commonly diagnosed cancer

and the second most common malignancy worldwide because of its high rates of tumor recurrence and metastasis, which cause a poor prognosis[2,3]. Systemic treatments, including surgery, chemotherapeutics and targeted therapeutics, have reached a bottleneck for improving patient prognosis. Immunotherapies, such as programmed death-1 (PD-1) and cytotoxic T-lymphocyte antigen 4 (CTLA-4) inhibitors, have transformed the treatment landscape for CRC patients and become important treatments, especially for advanced CRC patients with microsatellite instability-high (MSI-H) disease, which is highly infiltrated with immune cells and carries high neoantigen load[4]. Because of the low rate of CRC patients with MSI-H disease, the achievement of a complete response with immunotherapy is rare in the majority of CRC cases[5].

Necroptosis is an evolutionary form of caspase-independent programmed necrosis that is a vital process in the life cycle of organisms and contributes to the innate immune response by inducing tumor cell death. Necroptosis has emerged as a therapeutic target, as it creates dying cancer cells that can stimulate antitumor immune responses[6], and necroptosis activation can contribute to a clinically favorable immune signature and survival rates, highlighting the novel therapeutic possibility of combining a necroptosis-based therapeutic approach with immune checkpoint inhibitors for more efficient treatment of tumor patients. Necroptosis can enhance antitumor immunity more efficiently than can immunogenic apoptosis, implying the high potential of necroptosis as a therapeutic target in cancer[7]. Necroptosis induction significantly improves antitumor immunity by inducing the maturation of dendritic cells and activation of cytotoxic CD8+ T cells, which plays roles in antitumor immunity[8]. However, many factors, such as genetic instability, contribute to the resistance to necroptosis in CRC[9]. Han Qinrui reported that resibufogenin could suppress the growth and metastasis of CRC by inducing necroptosis in vivo[10]. Developing approaches to activate the necroptotic process and subsequently induce antitumor immune cells to exert antitumor effects may become a new direction for tumor immunotherapy.

Long noncoding RNAs (lncRNAs), which are not translated into proteins, can

regulate gene expression at multiple levels, such as the transcriptional, chromatin modification and post-transcriptional levels[11]. Furthermore, lncRNAs participate in various biological processes, such as stem cell pluripotency maintenance, cell cycle regulation and cell differentiation. Overexpression of some lncRNAs can inhibit the expression of necroptosis-related proteins and suppress the necroptotic pathway by downregulating membrane receptors, thereby reducing tumor cell necroptosis and antitumor immune cell infiltration[12]. In addition, lncRNAs interact with microRNAs (miRNAs) and affect the expression of other miRNA species. Experiments have confirmed that the lncRNA necrosis-related factor (NRF) targets miR-873 and RIPK1/RIPK3 to regulate cardiomyocyte necroptosis[13]. There are no reports on necroptosis-related lncRNAs widely mentioned as potential immunotherapeutic targets in CRC. Therefore, acquiring more knowledge on necroptosis-related lncRNAs and exploring the internal relationships and mechanisms of action these lncRNAs could help us understand the roles of necroptosis and lncRNAs in immunotherapy in CRC patients and explore more effective immunotherapeutic methods.

In this study, we aimed to explore the internal relationships and mechanisms of interaction between necroptosis-related lncRNAs and the tumor immune microenvironment (TME). As lncRNAs in bodily fluids are known to be new cancer biomarkers, we stratified CRC patients according to necroptosis-related lncRNAs, which allowed us to not only evaluate patient prognosis and improve precision medicine in clinical practice but also evaluate the efficacy of immunotherapy and guide the selection of immunotherapeutic methods. Additionally, we hoped to identify potential effective immunotherapeutic targets and drugs.

Materials and Methods

1 Acquisition of information for patients with CRC.

The entire analysis workflow is shown in Figure 1. To obtain RNA-sequencing data (HTSeq-Counts and HTSeq-FPKM) for colon adenocarcinoma (COAD), rectal adenocarcinoma (READ) and normal colorectal tissues, matching clinical data were downloaded from The Cancer Genome Atlas (TCGA). **The datasets analysed during**

the current study are available in the [The Cancer Genome Atlas (TCGA)] repository, [https://portal.gdc.cancer.gov/]. The training cohort was derived from the TCGA-CRC dataset, and the validation cohort was derived from clinical tissue samples from CRC patients (Table 1) who underwent surgery at the First Affiliated Hospital of Fujian Medical University between January 2018 and December 2018. Finally, 121 CRC patients who had complete clinical data and fresh pathological specimens stored in a freezer at -80°C were selected for inclusion in the validation cohort. This study was approved by the Ethics Committee of the First Affiliated Hospital of Fujian Medical University (NO. MRCTA, ECFAH of FMU[20190(21)]). **We identified the research was under the Ethics Committee approving including any relevant details; We also confirmed that all experiments were performed in accordance with relevant guidelines and regulations.**The FPKM values of the synthetic matrix were converted into TPM values with the data.table, dplyr, tidyr, and tibble R packages. As a result, we obtained two synthetic data matrices. The count value matrix was used to identify differentially expressed lncRNAs, while the TPM value matrix was used for the other analyses. We ultimately included 537 patients with relevant clinical information after excluding patients with missing overall survival (OS) values or short OS times (<30 days).

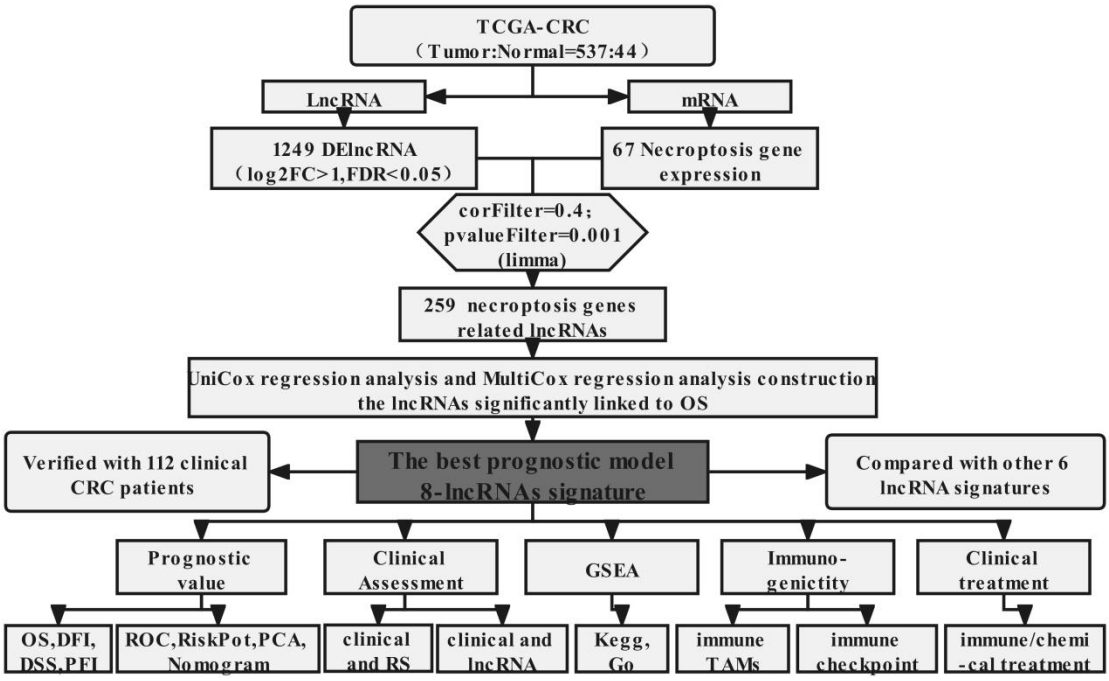

Figure 1. The entire analysis workflow for the study.

Table 1 Clinical characteristics of the colorectal cancer patients included in the study.

Characteristics	TCGA-CRC (n=537)			Clinical-CRC
	All	High risk (n=269)	Low risk (n=268)	(n=121)
Age				
≤65	234 (43.58%)	114 (42.38%)	120 (44.78%)	53 (43.8%)
>65	303 (56.42%)	155 (57.62%)	148 (55.22%)	68 (56.2)
Sex				
Male	287 (53.45%)	141 (52.42%)	146 (45.48%)	61 (50.41%)
Female	250 (46.55%)	128 (47.58%)	122 (45.52%)	60 (49.29%)
T stage				
T1	15 (2.94%)	8 (2.97%)	7 (2.61%)	3 (2.48%)
T2	93 (17.32%)	42 (15.61%)	51 (19.03%)	17 (14.05%)
T3	366 (68.16%)	180 (66.91%)	186 (69.40%)	49 (40.5%)
T4	63 (11.73%)	39 (14.50%)	24 (8.96%)	52 (42.98%)
N stage				
N0	316 (58.85%)	140 (52.04%)	176 (65.67%)	67 (55.37%)
N1	128 (23.84%)	67 (24.91%)	61 (22.76%)	31 (25.62%)
N2	92 (17.13%)	62 (23.05%)	30 (11.19%)	23 (19.01%)
Unknown	1 (0.19%)	0	1 (0.38%)	-
M stage				
M0	400 (74.49%)	190 (70.63%)	210 (78.36%)	102 (84.3%)
M1	75 (13.97%)	46 (17.1%)	29 (10.82%)	19 (15.7%)
Unknown	62 (11.55%)	33 (12.27%)	29 (10.82%)	-
Stage				
Stage I	93 (17.32%)	41 (15.24%)	52 (19.40%)	20 (16.53%)
Stage II	209 (38.92%)	91 (33.83%)	118 (44.03%)	42 (34.71%)
Stage III	149 (27.75%)	83 (30.86%)	66 (24.63%)	40 (33.06%)
Stage IV	76 (14.15%)	47 (17.47%)	29 (10.82%)	19 (15.7%)
Unknown	10 (1.86%)	7 (2.6%)	3 (1.12%)	-

2 Identification of necroptosis-related lncRNAs.

In total, 1249 differentially expressed lncRNAs (log2-fold change (FC) > 1, false

discovery rate (FDR) < 0.05, and p < 0.05) were identified after screening the synthetic data matrix with the limma R package and Strawberry Perl. The 67 necroptosis-related genes contained the M24779.gmt gene set included eight necroptosis-related genes, which was downloaded from the Gene Set Enrichment Analysis (GSEA) website (http://www.gsea-msigdb.org/gsea/index.jsp) and 59 genes reported in a previous article[14] (Table S 1). Then, 259 necroptosis-related lncRNAs with a Pearson correlation coefficient >0.4 and p< 0.001 were collected after correlation analysis was performed between the necroptosis-related genes and differentially expressed lncRNAs using the limma R package.

3 Development and preliminary validation of the risk signature.

Necroptosis-related lncRNAs were selected as candidate prognostic factors after univariate Cox analysis (uni-Cox) was performed and identified OS-related indicators with a p value < 0.05. Next, multivariate Cox analysis (multi-Cox) was used to construct a signature with the coefficients of the lncRNAs. We calculated the risk score (RS) as follows: RS=coefficient*exp lncRNA1+coefficient*exp lncRNA2+oefficient*exp lncRNA3+....+coefficient*exp lncRNAn. According to the median RS, subgroups including low- and high-risk groups were established[12, 13]. We used the chi-square test to analyze the relationships between the model and clinical factors to evaluate the prognostic value of the constructed model.

4 Validation of the lncRNA signature.

The differences in OS, disease-free survival (DFS), disease-free interval (DFI) and progression-free interval (PFI) between the low- and high-risk groups were analyzed using Kaplan–Meier (K-M) survival analysis and the "survival" and "survminer" R packages. Principal component analysis (PCA) was used to explore the distributions of the different groups. The RS and clinical characteristics were evaluated with uni-Cox and multi-Cox regression analyses to evaluate the independent factors. The 1-, 3-, and 5-year time-dependent, clinical characteristic and mixed RS receiver operating characteristic (ROC) curves of the model were plotted with the calculation procedure to evaluate the predicted outcome.

5 Verification of the predicted result of the nomogram.

The nomograms for the 1-, 3-, and 5-year OS and correction curves based on the Hosmer–Lemeshow test, which were built with the RS, the clinical model (age, sex, and TNM stage) and the combination model (age, sex, stage and RS) were used to verify the predicted results.

6 GSEA.

Gene Ontology (GO, go.v7.4.symbols.gmt) and Kyoto Encyclopedia of Genes and Genomes (KEGG, kegg.v7.4.symbols.gmt) analyses were performed with GSEA software to identify the significantly enriched pathways between the high-risk and low-risk groups. An FDR<0.25, P <0.05, and |enrichment score (ES)| > 0.3 were set as the cutoff criteria.

7 Analyses of ESTIMATE results, the TME and immune checkpoints.

After preparation for immune analyses, differential cluster analyses of the ESTIMATE score, stromal score, immune score, and tumor purity score were performed to compare the high- and low-risk groups based on the results of the ESTIMATE algorithm (using the “limma” and “vioplot” R packages). We calculated the immune infiltration statuses of CRC patients in the TCGA dataset, including the statuses indicated by analyses with TIMER, CIBERSORT, CBIERSORT-ABS, MCPCOUNTER, XCELL and EPIC, by using TIMER2.0 (http://timer.cistrome.org/). Then, we compared immune checkpoint activation between the high- and low-risk groups with the ggpubr R package.

8 Exploration of immunotherapy and drug predictions.

The TCGA-CRC gene expression profile and the high- and low-risk group information were used as inputs with the R software package “PRRophetic” to predict half-maximal inhibitory concentration (IC50) values with Genomics of Drug Sensitivity in Cancer (GDSC) (https://www.cancerrxgene.org/)[15].

9 Comparison of the lncRNA signature with other CRC prognostic signatures.

By reviewing the literature, we identified six different lncRNA-based risk models including the immune-related lncRNA signature (PMID: 30396175)[16], N6-methyladenosine-related lncRNA signature (PMID: 33959151)[17], autophagy-related lncRNA signature (PMID: 34745388)[18], fatty acid

metabolism-related lncRNA signature (PMID: 34692467)[19], epithelial-mesenchymal transition-related lncRNA signature (PMID: 33898515)[20] and tumor mutational burden-related lncRNA signature (PMID: 33958876)[21] for comparison with our lncRNA signature. To make the models comparable, we calculated each RS according to the RS calculation formula provided by the model based on the corresponding gene expression in the same TCGA-CRC patient cohort. Then, we evaluated the 1-, 3-, and 5-year time-dependent ROC curves of the six models according to the RS.

10 Validation of the lncRNA signature in clinical CRC patients with real-time quantitative PCR.

We first used real-time PCR to test the expression of the lncRNAs in the signature and verified the lncRNA expression in 121 clinical CRC patients. The steps of RNA extraction (ER501-01, TransGen Biotech, Beijing, China), reverse transcription (AE341-02, TransGen Biotech, Beijing, China) and amplification were carried out in accordance with the manufacturer's instructions. The primer sequences for all lncRNAs and the internal reference gene GAPDH are shown in Table S 3. Then, we calculated RSs according to the RS calculation formula for our model. The 1-, 2- and 3-year time-dependent, clinical characteristic and mixed RS ROC curves and the K-M survival curve were plotted to validate the predictive ability of the 8-lncRNA signature.

11 Statistical analysis.

All statistical analyses were performed using R software (version 4.1.2). An lncRNA and necroptosis-related gene coexpression network was drawn using Cytoscape software (version 3.9.0). The performance of the model was evaluated with K-M curves, time-dependent ROC analysis and Cox regression analysis. A two-tailed $P < 0.05$ was considered statistically significant.

Results

1 Necroptosis-related lncRNAs in TCGA-CRC patients.

All the clinicopathologic characteristics of the CRC patients included in this study are shown in Table 2. The expression of 67 necroptosis-related genes (Figure

2A) and 14,142 lncRNAs was identified from the TCGA dataset. The 1249 differentially expressed lncRNAs (log2-FC > 1, FDR < 0.05, and p < 0.05) (Figure 2B) included 1075 upregulated and 174 downregulated lncRNAs (Figure 2C). Finally, the 259 necroptosis-related lncRNAs with a Pearson correlation coefficient >0.4 and p< 0.001 were selected. The network figure and corresponding data connecting the necroptosis-related genes and lncRNAs are shown in Figure 2D and Table S1.

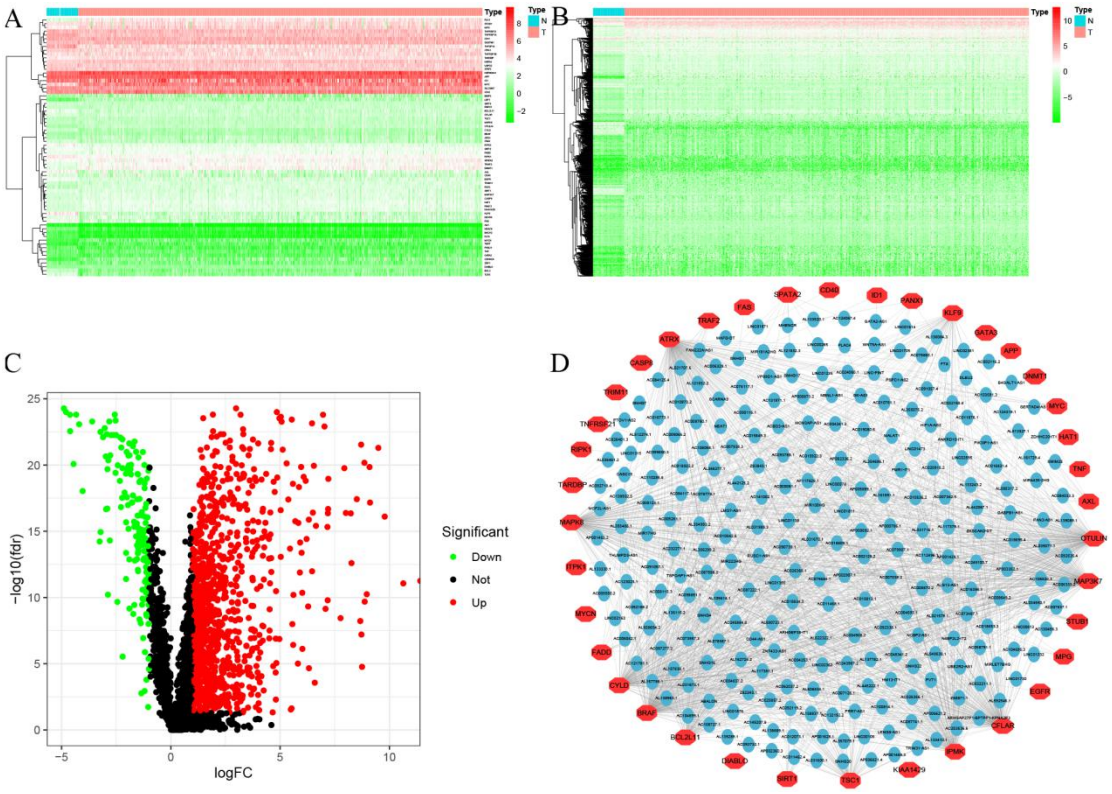

Figure 2. Necroptosis-related gene and lncRNA expression. **A** Heatmap of the expression of 67 necroptosis-related genes. **B** Heatmap of the expression of 1249 necroptosis-related lncRNAs. **C** Volcano plot of the differentially expressed necroptosis-related lncRNAs. **D** The network connecting the necroptosis-related genes and lncRNAs (correlation coefficient>0.4 and p<0.001).

2 Model construction.

There were 29 necroptosis-related lncRNAs significantly correlated with OS according to uni-Cox regression analysis (Figure 3A). The results showed that the p values of the hazard ratios (HRs) for these 26 lncRNAs were all less than 0.05 (Table S 4), indicating that their high expression might be related to a poor prognosis in CRC. After including other confounders in the multi-Cox regression analysis, the RS was still an independent prognostic indicator for OS (Figure 3B, Table 2). In addition, we

found that 5 lncRNAs were upregulated and the others were downregulated, as indicated in the Sankey diagram (Figure 3C). We calculated the RS with the following formula:

RS=AP001469.3×(0.3955)+AC007128.1×(0.4998)+LINC02381×(0.3903)+AC099850.3×(-0.2919)+AC010973.2×(0.7757)+MIR4435-2HG×(0.7466)+AC245100.7×(0.4713)+AL137782.1×(-1.1265).

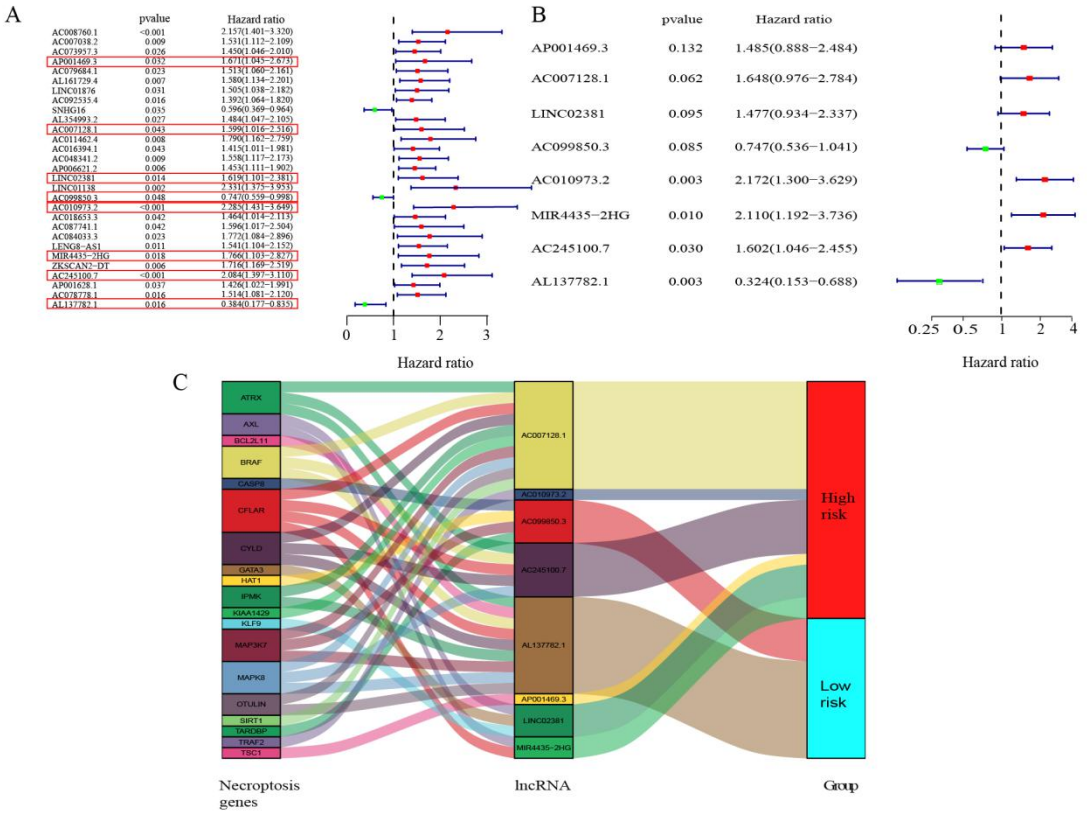

Figure 3. Construction of a signature including 8 necroptosis-related lncRNAs that was associated with OS in CRC. **A** Necroptosis-related lncRNAs significantly correlated with OS by uni-Cox regression analysis ($p<0.05$). **B** Multi-Cox regression analysis results showing that the 8 necroptosis-related lncRNAs could be used to evaluate CRC prognosis. **C** Sankey diagram of the necroptosis-related genes and lncRNAs.

Table 2 Univariate and multivariate Cox regression analyses of necroptosis-related lncRNAs in colorectal cancer

Variables	Univariate analysis		Multivariate analysis		
	HR (95% CI)	P value	Coefficient	HR (95% CI)	P value
AP001469.3	1.671 (1.045-2.673)	0.032	0.396	1.485 (0.888-2.484)	0.132
AC007128.1	1.599 (1.016-2.516)	0.043	0.500	1.648 (0.976-2.784)	0.062
LINC02381	1.619 (1.1.1-2.381)	0.014	0.390	1.477 (0.934-2.337)	0.095
AC099850.3	0.747 (0.559-0.998)	0.048	-0.292	0.747 (0.536-1.041)	0.085
AC010973.2	2.285 (1.431-3.649)	0.001	0.776	2.172 (1.3-3.629)	0.003
MIR4435-2HG	1.766 (1.103-2.827)	0.018	0.747	2.110 (1.192-3.736)	0.010
AC245100.7	2.084 (1.397-3.110)	0.000	0.471	1.602 (1.046-2.455)	0.030
AL137782.1	0.384 (0.177-0.835)	0.016	-1.127	0.324 (0.153-0.688)	0.003

3 Verification and assessment of the model.

Patients were divided into low-risk (n=268) and high-risk (n=269) groups with an optimal cutoff value of 0.9558 for the RS, and the clinicopathological characteristics of the two groups are shown in Table 2. As the RS increased, the patient mortality risk increased gradually, while the survival risk decreased gradually (Figure 4A, B). In addition, different conventional clinicopathological characteristics, such as age, sex, and TNM stage, were compared between the two groups. The high-risk group had not only a higher mortality rate but also a higher N grade, M grade and stage, with greater lymph node and distant metastasis rates (Figure 4C). PCA was used to compare the efficiencies of different gene set groups (all genes, differentially expressed lncRNAs, necroptosis-related genes, all necroptosis-related lncRNAs and our signature lncRNAs) in separating CRC patients. We found that our necroptosis-related lncRNA signature could best distribute CRC patients into the high- and low-risk groups (Figure 5A-E).

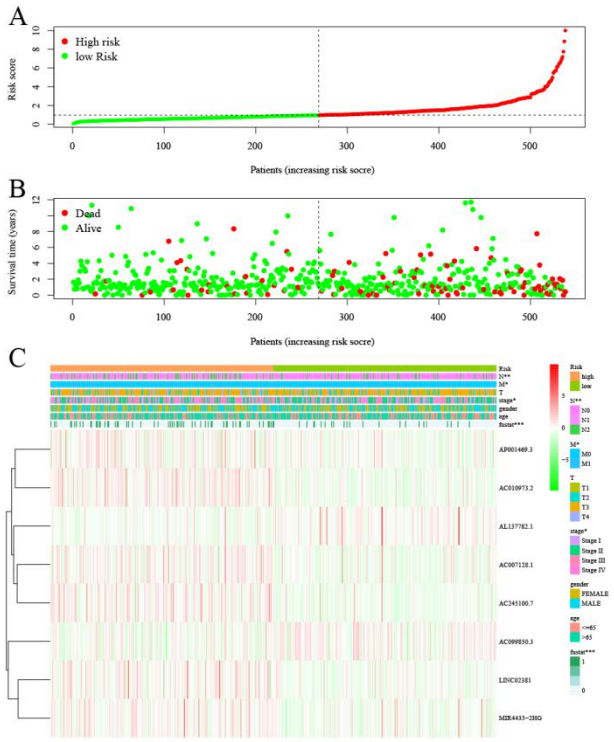

Figure 4. Prognostic value of the signature containing 8 necroptosis-related lncRNAs for the TCGA-CRC cohort. **A** Exhibition of the necroptosis-related lncRNA signature based on the risk score. **B** Survival time and survival status comparisons between the high- and low-risk groups. **C** Heatmap of the expression of 8 lncRNAs in the different groups and the relationships between clinicopathological characteristics and the RS. * $p<0.05$, ** $p<0.01$, *** $p<0.001$.

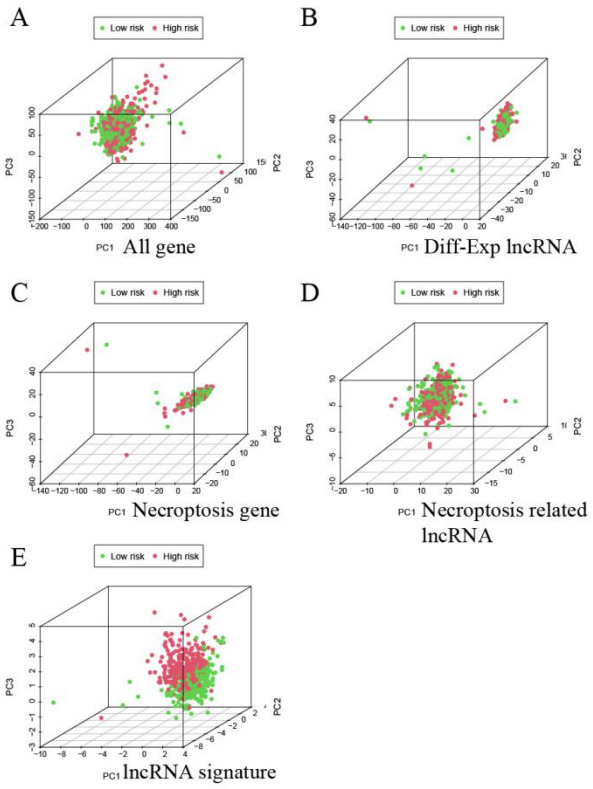

Figure 5. PCA was used to compare the efficiencies of models constructed based on different gene sets in stratifying the OS of CRC patients. **A** Models constructed based on all genes. B Models constructed based on differentially expressed lncRNAs. **C** Models constructed based on necroptosis-related genes. **D** Models constructed based on all necroptosis-related lncRNAs. **E** Models constructed based on our signature lncRNAs.

The OS of the high-risk group was significantly poorer than that of the low-risk group ($p<0.0001$; Figure 6A), and the DSS and PFI of the high-risk group were significantly poorer than those of the low-risk group ($p<0.01$; Figure 6B, C). Furthermore, the DFI was significantly different between the high-risk group and the low-risk group ($p>0.05$; Figure 6D). All of the K-M analysis results showed that the CRC patients in the high-risk group had a poorer prognosis and shorter OS, DSS, and PFI. The areas under the ROC curve (AUCs) of the RSs for 1-, 3- and 5-year OS were 0.79, 0.81 and 0.77, respectively, (Figure 6E), and the AUC of the RS for 1-year OS was higher than the AUC of any other clinicopathological characteristic, such as age, sex, tumor invasion depth (T stage), lymph node metastasis (N stage), or distant metastasis (M stage) (Figure 6F). All of these results indicate that the model is

moderately sensitive and specific for predicting the prognosis of CRC patients.

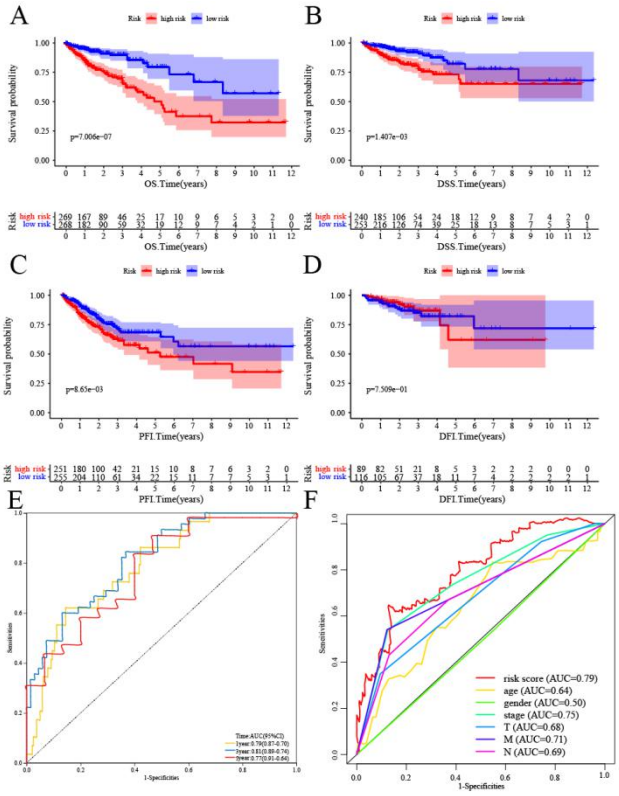

Figure 6. Prognostic value of the signature including 8 necroptosis-related lncRNAs evaluated with K-M survival curves and ROC curves. **A** The K-M survival curves for the OS of patients in the high- and low-risk groups. **B** The K-M survival curves for the DSS of patients in the high- and low-risk groups. **C** The K-M survival curves for the PFI of patients in the high- and low-risk groups. **D** The K-M survival curves for the DFI of patients in the high- and low-risk groups. **E** The areas under the ROC curve (AUCs) of the RSs for 1-, 3- and 5-year OS. **F** The AUCs of the RS for 1-year OS and for clinicopathological characteristics.

To further explore the prognostic value of the necroptosis-related lncRNA signature for CRC patients stratified by clinicopathological characteristics, we divided patients into different groups according to age, sex, T stage, N stage, M stage or total stage, and the results showed that the RS of CRC patients was positively associated with N stage, M stage and total stage but not significantly correlated with age, sex or T stage in the different stratified analyses (Figure 7A-D).

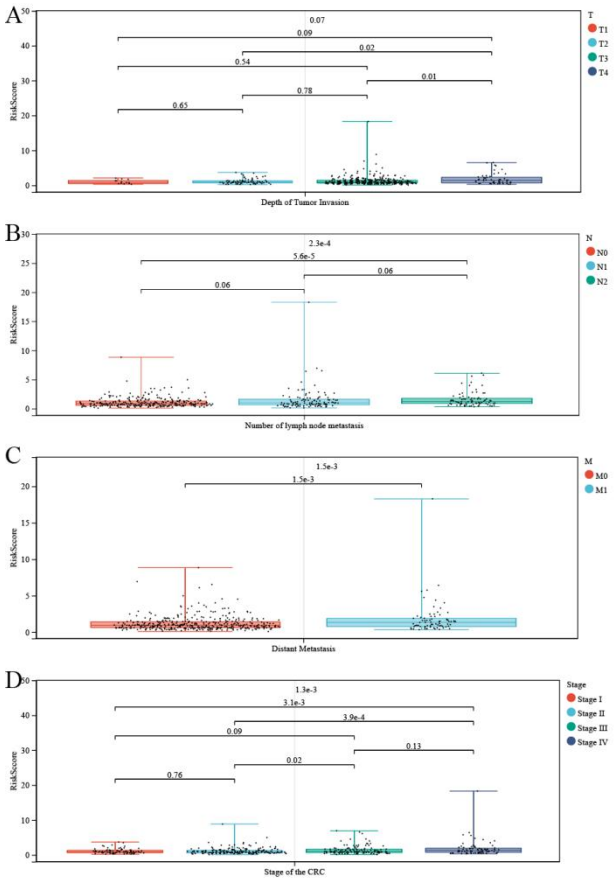

Figure 7. The prognostic value of the necroptosis-related lncRNA signature for CRC patients stratified by clinicopathological characteristics. **A** The differences in the RS for different T stages. **B** The differences in the RS for different N stages. **C** The differences in the RS for different M stages. **D** The differences in the RS for different total stages.

4 Construction of a predictive nomogram for CRC.

The HR for the RS and 95% confidence interval (CI) calculated by uni-Cox regression analysis were 1.309 and 1.222-1.403 ($p<0.001$), respectively (Figure 8A), and those calculated by multi-Cox regression analysis were 1.214 and 1.123-1.312 ($p<0.001$), respectively. In addition, age (1.030, 1.009-1.080; $p=0.005$) and T stage (1.750, 1.082-2.831; $p =0.023$) were the other two independent prognostic parameters (Figure 8B) identified by multi-Cox regression analysis. Then, we built a nomogram for predicting the 1-, 3-, and 5-year OS rates of CRC patients according to these three independent prognostic factors (RS, age, and T stage) (Figure 8C). Calibration plots showed that the performance of the nomogram was best in predicting 1-, 3- and 5-year OS (Figure 8D) and that the total RS of the nomogram could clearly divide the

high- and low-risk groups; the high-risk group had a poorer prognosis by K-M analysis (Figure 8E). The AUCs of the total RSs for 1-, 3- and 5-year OS were 0.76, 0.84 and 0.86, respectively (Figure 8F).

In conclusion, our predictive model may increase the predictive sensitivity and specificity of traditional clinical models and provide some information that may be helpful in the clinical prognostic assessment and best management of CRC patients.

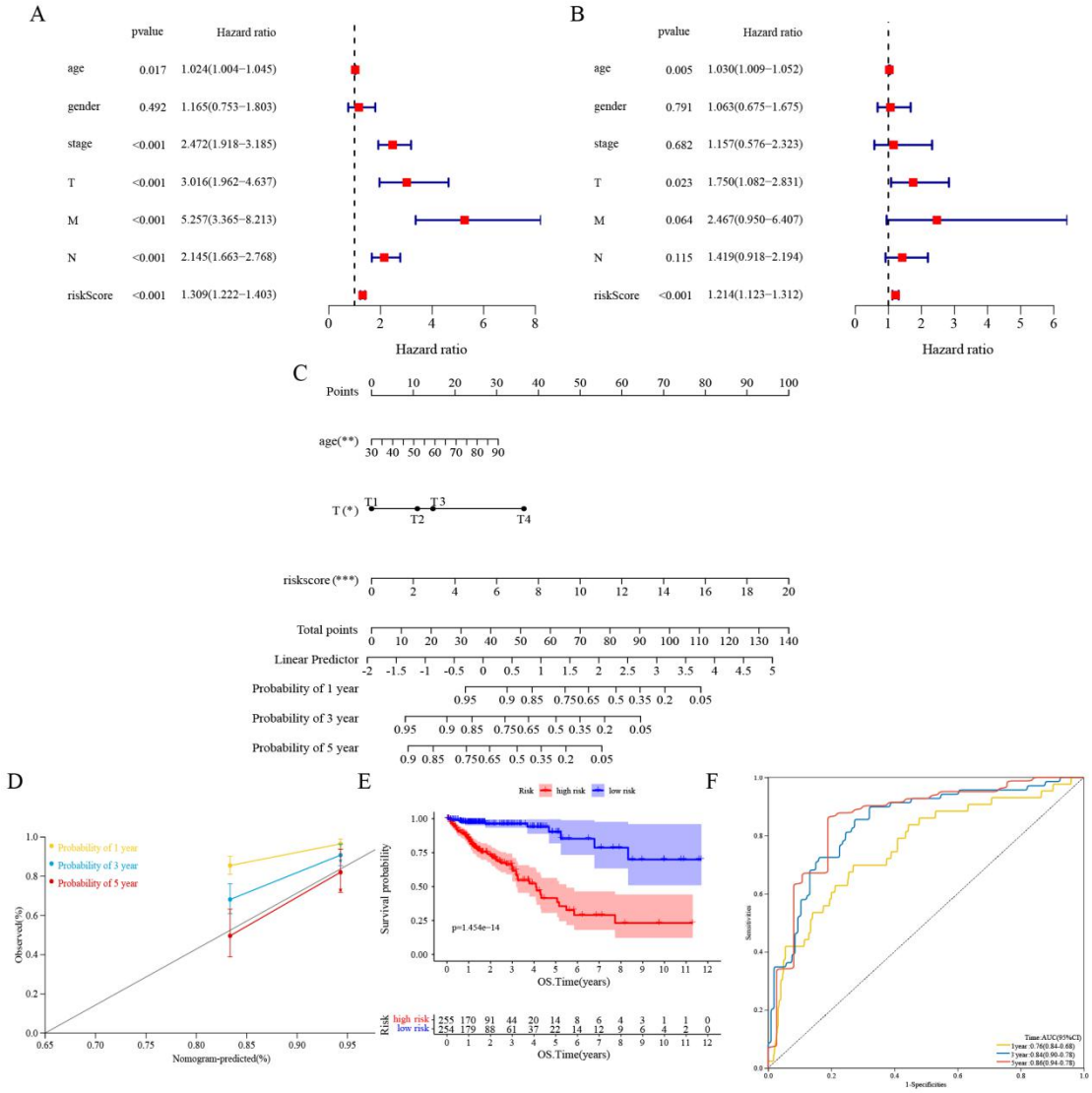

Figure 8. Construction of the predictive nomogram and assessment of the signature. **A** Uni-Cox regression analyses of clinical factors and the RS for OS. **B** Multi-Cox regression analyses of clinical factors and the RS for OS. **C** The nomogram that integrated age, RS and T stage predicted the probabilities of 1-, 3-, and 5-year OS in CRC. **D** The calibration curves for 1-, 3-, and 5-year OS. **E** The K-M OS curves of patients stratified into the high- and low-risk groups with the cutoff

for the nomogram total score. **F** The 1-, 3-, and 5-year ROC curves for the nomogram total score.

5 Advantage of the signature versus other prognostic lncRNA signatures in CRC.

There were many lncRNA-related models that have been derived from the TCGA database for predicting the prognosis of CRC patients, such as the immune-related lncRNA signature, N6-methyladenosine-related lncRNA signature and autophagy-related lncRNA signature. The AUCs for 1-, 3- and 5-year OS were 0.59, 0.56 and 0.60 for the immune-related lncRNA signature; 0.67, 0.69 and 0.65 for the N6-methyladenosine-related lncRNA signature; 0.71, 0.72 and 0.74 for the autophagy-related lncRNA signature; 0.74, 0.74 and 0.76 for the fatty acid metabolism-related lncRNA signature; 0.62, 0.65 and 0.56 for the epithelial-mesenchymal transition-related lncRNA signature; and 0.55, 0.54 and 0.50 for the tumor mutational burden-related lncRNA signature, respectively (Figure 9A-F). Most of these AUCs for 1-, 3- and 5-year OS were lower than those for the necroptosis-related lncRNA signature, which had better prognostic efficacy.

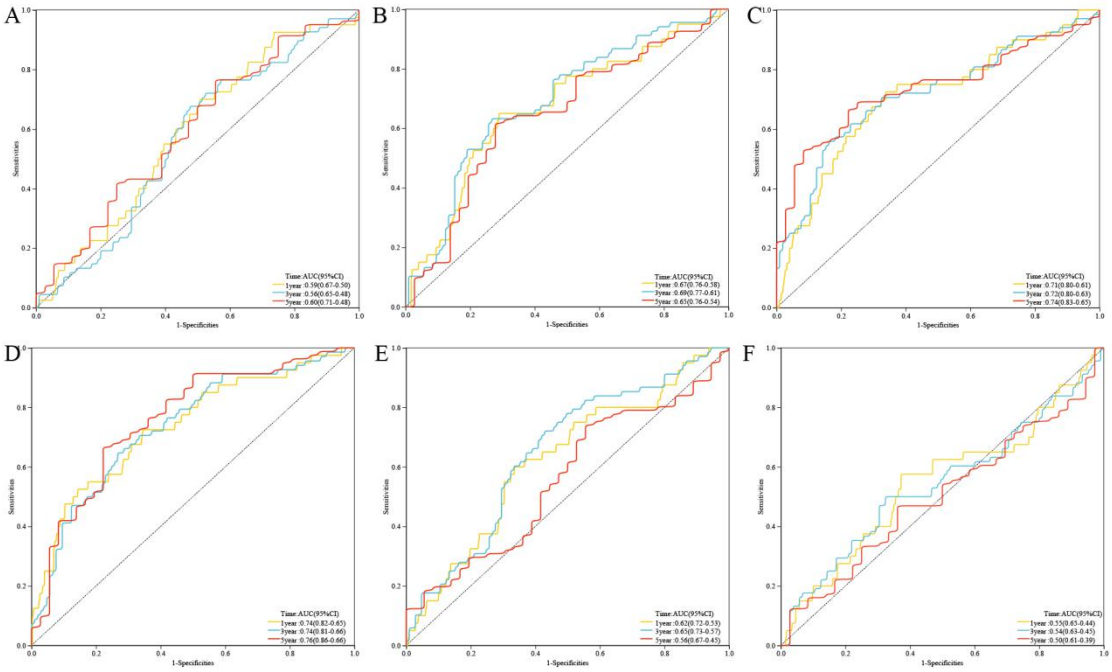

Figure 9. Comparison of the signature with other prognostic lncRNA signatures for CRC. **A** The AUCs for 1-, 3- and 5-year OS for the immune-related lncRNA signature. **B** The AUCs for the N6-methyladenosine-related lncRNA signature. **C** The AUCs for the autophagy-related lncRNA signature. **D** The AUCs for the fatty acid metabolism-related lncRNA signature. **E** The AUCs for

the epithelial-mesenchymal transition-related lncRNA signature. **F** The AUCs for the tumor mutational burden-related lncRNA signature.

6 Assessment of the signature and the relationships between lncRNAs and clinical characteristics in the clinical-CRC cohort.

The AUCs for 1-, 2- and 3-year OS were 0.74, 0.68 and 0.66, respectively, for the CRC patients with clinical data, which were all higher than 0.65 and suggested that this model could be used to predict the prognosis of CRC patients (Figure 10A). The AUC for the clinical data RS for 1-year OS was higher than the AUC for any other clinicopathological characteristic, such as age, sex, T stage, N stage, M stage, or total stage (Figure 10B). OS was significantly poorer in the high-risk group (n=61) than in the low-risk group (n=60), which were defined by the median RS as the cutoff ($p<0.01$, Figure 10C).

In the clinical-CRC cohort, the clinical value of RS with the multiple clinical characteristics was examined by uni-Cox and multi-Cox regression analysis. The HR for the RS and 95% confidence interval (CI) calculated by uni-Cox regression analysis were 54.17 and 5.99−490.03 ($p<0.001$), respectively (Figure S4A), and those calculated by multi-Cox regression analysis were 39.43 and 54.71−330.12 ($p<0.001$), respectively. In addition, age (1.032, 1.006−1.059; $p=0.014$) was the other independent prognostic parameters (Figure S4B) identified by multi-Cox regression analysis. The AC099850.3 and AL137782.1 showed as a protective factor significantly associated with better OS of the CRC patients, and the other lncRNAs were also showed as a risk factor with significantly poorer OS with the best expression cut-off point in the K-M method (Figure S4C-J). In a word, most of the have the the prognostic values in the clinical-CRC cohort patients.

Then, the expression levels of the 8 lncRNAs were stratified by clinicopathological characteristics, and we found that the expression of AC007128.1, MIR4435-2HG and AC245100.7 was related to N stage, M stage and total stage (all $p< 0.05$). The expression of LINC02381 was related to N stage, and the expression of AP001469.3 was related to M stage (all $p<0.05$), but none of the 8 lncRNAs were related to age, sex or T stage in the TCGA-CRC cohort (Figure 10D-G). In the clinical

CRC patient cohort, the RSs were significantly related to T stage, N stage, M stage and total stage. The expression of AC007128.1, AP001469.3 and MIR4435-2HG was related to N stage, M stage and total stage, and MIR4435-2HG was also related to T stage (all $p<0.05$). The expression of AC245100.7 was related to M stage ($p<0.05$), but the other lncRNAs were not related to any of the clinicopathological characteristics (Figure 10H-K, Figure S1).

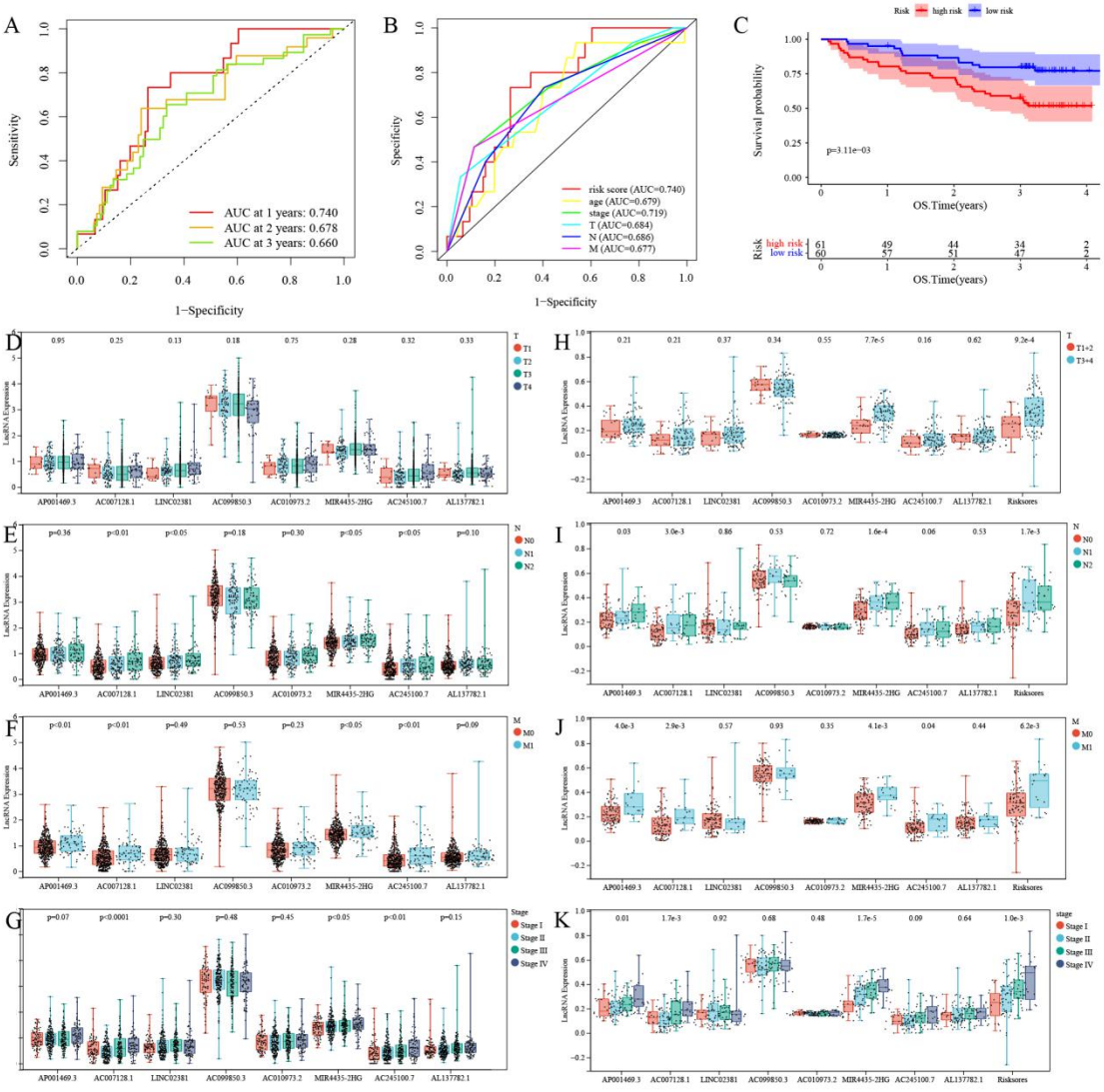

Figure 10. Assessment of the signature in the clinical CRC cohort and the relationships between the 8 lncRNAs and clinicopathological characteristics. **A** The AUCs for 1-, 2- and 3-year OS determined with the clinical data of CRC patients. **B** The AUCs for the RS of 1-year OS and for clinicopathologic characteristics. **C** The K-M survival curves for the OS of the high- and low-risk groups, which were defined by the median RS as the cutoff. **D-G** The relationships between the 8

lncRNAs and clinicopathological characteristics in the TCGA-CRC cohort. **H-K** The relationships between the 8 lncRNAs and clinicopathological characteristics in the clinical CRC cohort.

7 GSEA.

GSEA results showed that the top ten enriched KEGG terms in the high-risk patient group were in cancer- and tumor metastasis-related pathways, such as “basal cell carcinoma”, “complement and coagulation cascades”, “ECM receptor interaction” and “focal adhesion” (Figure 11A-D). The top ten enriched GO terms in the high-risk patient group were tumor metastasis- and ion channel-related pathways, such as “regulation of calcium ion transmembrane transport”[22], “collagen containing extracellular matrix”, “ciliary tip” and “negative regulation of transcription regulatory region DNA binding” (Figure 11E-H, Table S 5). These main pathways might be associated with the poorer prognosis of the high-risk group.

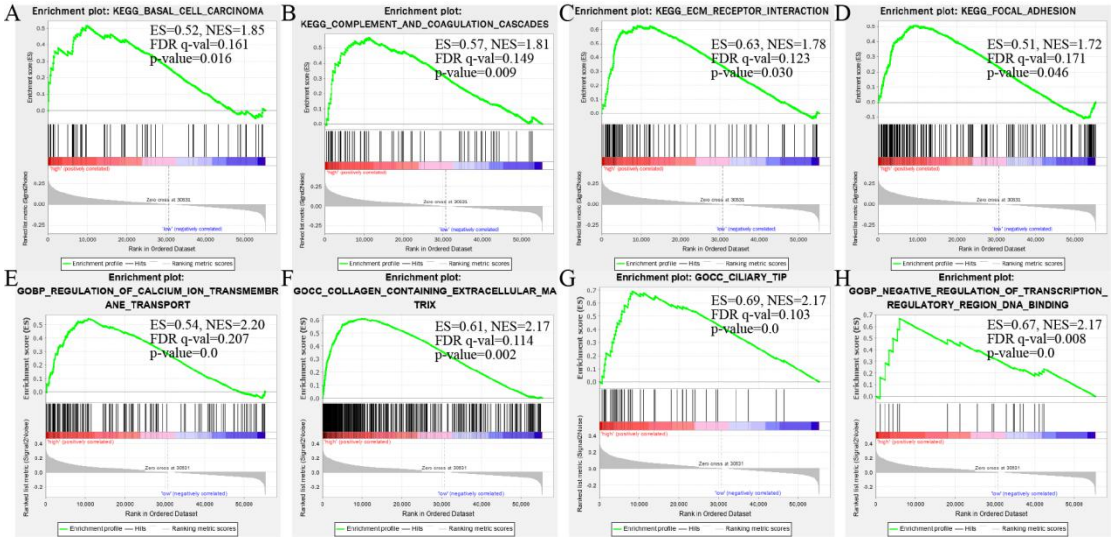

Figure 11. GSEA results. **A** The main enriched KEGG terms in the high-risk group included “basal cell carcinoma”, “complement and coagulation cascades”, and “ECM receptor interaction”. **B** The main enriched KEGG terms in the high-risk group included “regulation of calcium ion transmembrane transport”, “collagen containing extracellular matrix”, and “ciliary tip”.

8 Investigation of immune factors and clinical treatment in the risk groups.

The differences in immune cell infiltration and the TME between the different RS groups were analyzed. ESTIMATE analysis results showed that the high-risk group had a higher ESTIMATE (microenvironment) score, immune score and stromal score but a lower tumor purity than the low-risk group (all $p< 0.001$), which signified

different TMEs in the two groups (Figure 12A-D). The heatmap (Figure 12E) for immune cell infiltration showed that more immune cells were associated with the high-risk group on different platforms (Table S6); the immune cell populations included CD4+ memory T cells, CD4+ Th2 cells, CD8+ central memory T cells, NKT cells, regulatory T cells (Tregs) and B cells identified by XCELL (Figure 12F-K); CD4+ T cells and M2 macrophages identified by TIMER; activated CD4+ memory T cells identified by CIBERSORT; and M2 macrophages identified by CIBERSORT−ABS (all $p<0.05$) (Figure S2). In addition, we found more significantly reduced numbers of antitumor immune cells, such as CD4+ Th2 cells, CD8+ central memory T cells, NKT cells, Tregs and B cells (Figure 12F-K)[23], and increased numbers of protumor immune cells, such as cancer-associated fibroblasts (CAFs), hematopoietic stem cells, M0 macrophages and M2 macrophages[24], in the tumor microenvironment of the high-risk group, which suggested a poor prognosis and might be a direction for immunotherapy in CRC (Figure 12L-O)[25].

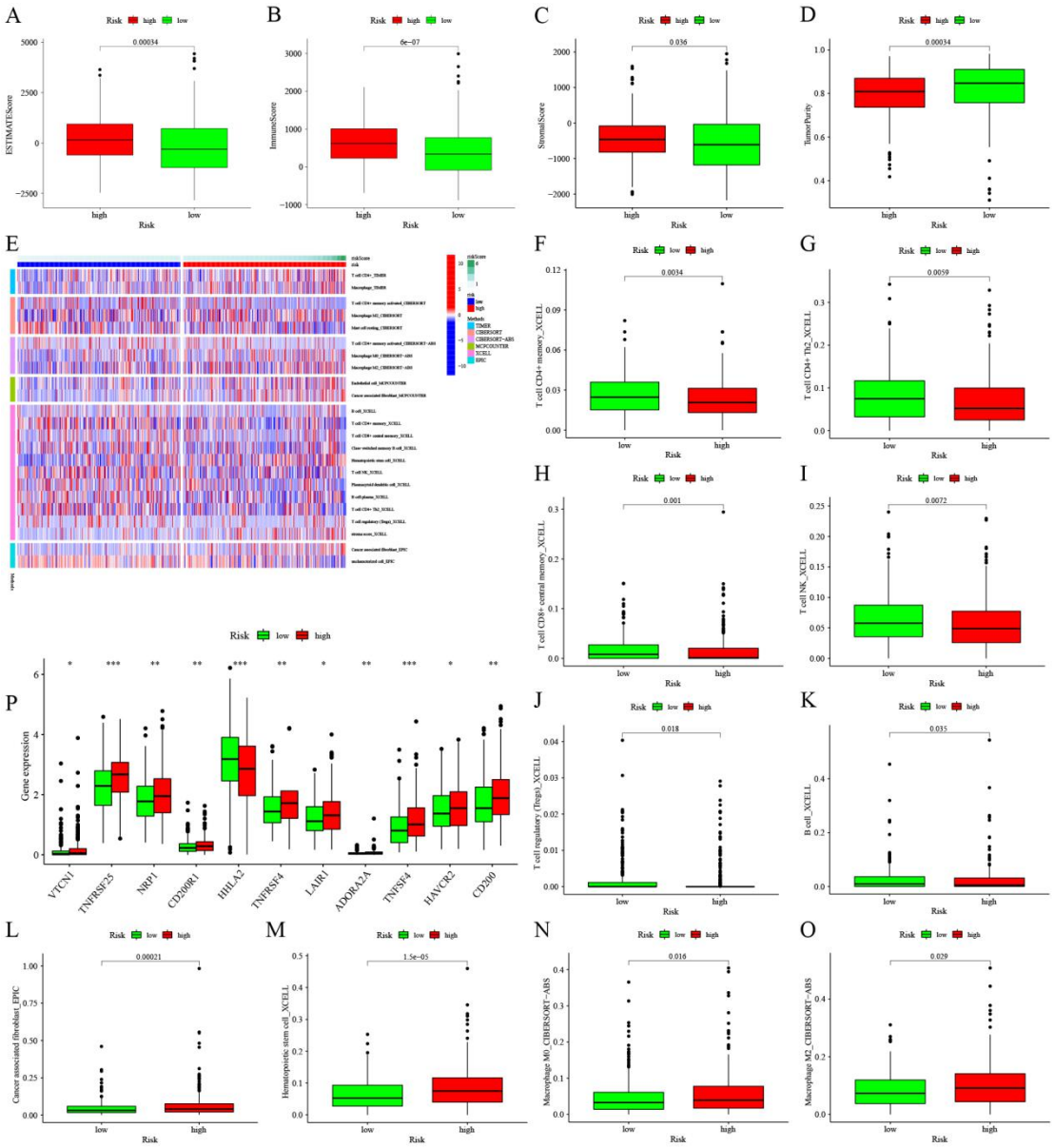

Figure 12. Investigation of the tumor immune microenvironment (TME). **A** Comparison of ESTIMATE scores between the low- and high-risk groups. **B** The comparison of immune scores between the low- and high-risk groups. **C** Comparison of stomal scores between the low- and high-risk groups. **D** Comparison of tumor purity between the low- and high-risk groups. **E** Heatmap of immune cell infiltration showing that more immune cells were associated with the high-risk group on different platforms. **F-K** More significantly reduced numbers of antitumor immune cells

in the TME in the high-risk group. **L-O** More significantly increased numbers of protumor immune cells in the TME in the high-risk group. **P** Differences in the expression of 11 checkpoint molecules between the high- and low-risk groups.

Most immune checkpoint molecules, such as VTCN1[26], TNFRSF25 and NRP1, also showed greater activation in the high-risk group (Figure 12P), which implied that we could choose appropriate checkpoint inhibitors for CRC patients. Moreover, we found that 16 immunotherapeutic anticancer drugs and 22 chemotherapeutic or targeted drugs showed lower IC50 values in the high-risk group when applied for CRC therapy (Figure 13A, B; Figures S2 and S3)[27]. These observations will assist in the discovery of potential drugs for effective antitumor immunotherapy and chemotherapy to improve the therapeutic efficacy and prognosis of patients in high-risk groups.

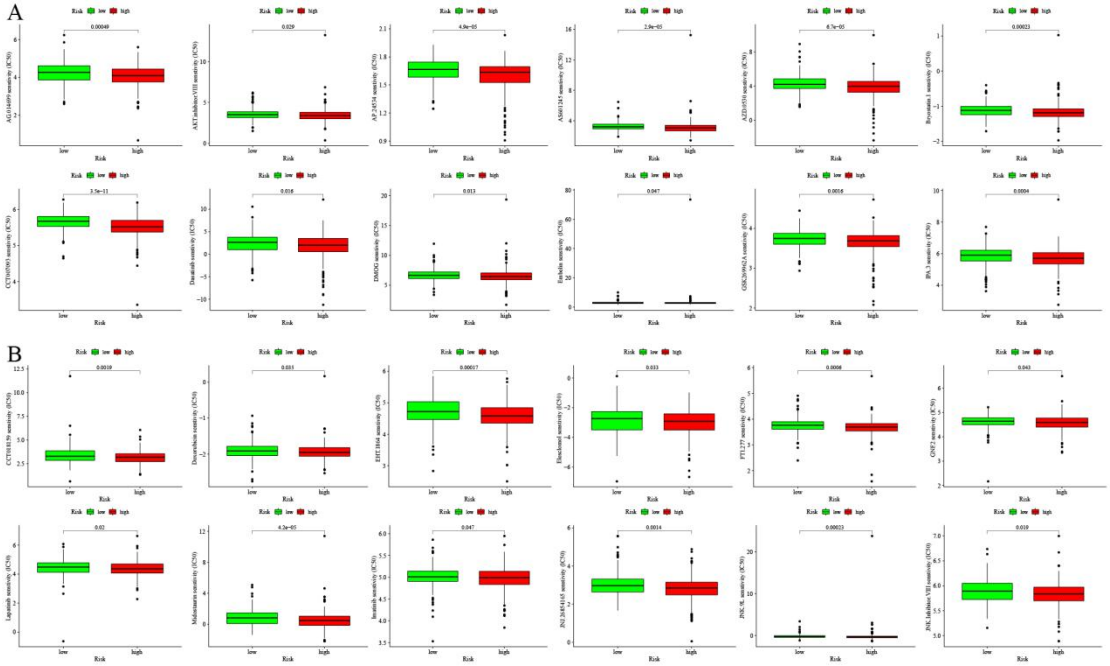

Figure 13. Anticancer drug prediction for the risk groups. **A** Potential drugs for effective antitumor immunotherapy in the high-risk group. B Potential drugs for effective antitumor chemotherapy in the high-risk group.

Discussion

In recent years, an increasing number of novel lncRNAs have been identified, and the roles of lncRNAs in CRC development have been increasingly studied[11]. In our previous study, we showed the effectiveness of lncRNA signatures in prognostic prediction based on the immune environment and identified the role of H19 in colon cancer[28]. There are many lncRNA-related models for predicting the prognosis of CRC patients based on the TCGA database, such as the immune-related lncRNA

signature, N6-methyladenosine-related lncRNA signature and autophagy-related lncRNA signature. Here, we identified a new model including 8 necroptosis-related lncRNAs that was associated with CRC OS and widely mentioned as a potential immunotherapeutic target in CRC. The fidelity of this model was tested with clinical datasets and compared with that of other models. Molecular signatures are considered a favorable tool for disease stratification, but a necroptosis-related lncRNA-based signature is still lacking in CRC. Two necroptosis-related lncRNA signatures were identified in gastric cancer (GC)[29], supporting that such a signature could predict prognosis and help distinguish between cold and hot tumors for improving personalized therapy in GC.

In the present study, we developed a prognostic prediction model with eight necroptosis-related lncRNAs that could effectively distinguish CRC patients with different prognoses. Moreover, uni-Cox and multi-Cox analyses confirmed that this model was an independent prognostic risk factor, and the OS, DSS, PFI and PCA results illustrated that as the RS increased, the patient mortality risk increased gradually, while the survival risk decreased gradually. The discrimination potential of the RS was superior toother clinical prognostic risk factors (T stage, N stage, M stage and total stage). We also compared the prognostic performance of this model with that of previously reported prognostic biomarkers for CRC. The AUCs for OS results demonstrated that the necroptosis-related lncRNA signature had higher fidelity than 6 other signatures, including the immune-related lncRNA signature, N6-methyladenosine-related lncRNA signature and autophagy-related lncRNA signature[16-21]. This necroptosis-related lncRNA-based signature showed a perfect clustering capability and could be treated as a potential tool for CRC molecular signatures. Although the 8-lncRNA signature showed potential as a prognostic biomarker for CRC, other independent large clinical datasets need to be evaluated to assess the fidelity of this signature as a prognostic biomarker for CRC.

The RS was correlated with tumor staging, as well as the N stage and M stage, in the TCGA-CRC and clinical CRC cohorts. These results suggested that the poor prognosis of the high-risk group might be closely related to the high risks of lymph

node metastasis and distant metastasis and that this model would also be useful for detecting lymphatic metastasis, distant metastasis and total stage in CRC. Recent studies have revealed an important role for necroptosis in metastasis and implied the potential of targeting necroptosis with antimetastatic and advanced-stage cancer therapies[30]. Additionally, the GSEA results showed that most of the enriched KEGG and GO terms in the high-risk patient group were related to tumor metastasis-related pathways, implying the important role of necroptosis in CRC metastasis, which has received little attention and research to date[31,32]. The definite relationships between immune cell infiltration or function and metastasis in the TME indicate that we should pay much attention[33]. Necroptosis was found to be involved in antitumor immunity, possibly by altering TME functions during cancer immunotherapy[34]. Therefore, we carefully performed an in-depth review of the differences in the functional status of the TME and number of infiltrating immune cells between the high- and low-risk groups, aiming to explore the factors affecting prognosis and potential immunotherapeutic targets. The high-risk group had a high immune score, ESTIMATE score and stomal score, which are traditionally considered to indicate a “hot tumor” and stronger responses to immunotherapy[35]. However, the infiltrated immune cells and their functions are the most important factors in immunotherapy. The high-risk group was infiltrated with more immunosuppressive cells, such as CAFs[36], hematopoietic stem cells[37] and M2 macrophages[38,39], and fewer antitumor effector immune cells, such as CD8+ T cells[40] and Tregs[41], which may be the reason for the increased metastasis and poor prognosis in the high-risk group. However, selecting effective treatment methods and improving therapeutic efficacy in these high-risk patients remain difficult issues. Traditional immune checkpoint therapy has achieved only poor efficacy in CRC, and it is necessary to identify other potential therapeutic targets or develop combination therapies including immune checkpoint therapy as future directions for exploration. Our results found that increased potential immune checkpoint gene expression was closely related to the high-risk group, and more potential immunotherapeutic and chemotherapeutic drugs had lower IC50 values in the high-risk group than in the

low-risk group[42-45].

Finally, we found that the expression of the lncRNAs AC007128.1, MIR4435-2HG and AC245100.7 was related to N stage, M stage and total stage in the TCGA-CRC cohort, and the expression of AC007128.1, AP001469.3 and MIR4435-2HG was related to N stage, M stage and total stage in the clinical CRC cohort. MIR4435-2HG is relatively highly researched in CRC[46]; it likely plays poor prognostic roles and could be a potential therapeutic target in CRC[47]. MIR4435-2HG has been associated with AXL, which reprograms the immunological microenvironment when PD-1 inhibitors are administered as an immunotherapy[48]. AC007128.1 plays an important role and is associated with many necroptosis-related genes, such as MAPK8[49] and BRAF[50], that contribute to immunotherapy but has not been reported in CRC. AC007128.1 expression was upregulated and associated with a poor prognosis in esophageal squamous cell carcinoma (ESCC), which may promote epithelial-mesenchymal transition by increasing the activation of the MAPK/ERK and MAPK/p38 signaling pathways in ESCC cells[51]. However, AP001469.3 and AC245100.7 have not been reported in CRC or other cancers. Most of these lncRNAs may play crucial roles in necroptosis in CRC. However, the specific mechanism needs to be explored through more in-depth basic experiments.

Overall, we identified a necroptosis-related lncRNA signature for CRC prognosis prediction and subtyping using lncRNA expression profiles. This signature will not only greatly improve the ability to predict CRC prognosis but also allow exploration of the reasons and mechanism underlying the increased TME infiltration of more immunosuppressive cells and decreased TME infiltration of antitumor effector immune cells in high-risk group patients, which leads to distant metastases. This signature found additional potential immune checkpoint genes and immunotherapeutic and chemotherapeutic drugs, and future in-depth research will identify more potential biomarkers and treatment targets for CRC.

Supplementary Information

Appendix file1: Table S 1. The 67 necroptosis-related genes collected contained the

M24779.gmt gene set and 59 genes reported previously.

Additional file 2: Table S 2. Correlation coefficients between necroptosis-related genes and lncRNAs.

Additional file 3: Table S 3. Primer sequences for all lncRNAs and the internal reference gene GAPDH.

Additional file 4: Table S4. Necroptosis-related lncRNAs significantly correlated with OS according to uni-Cox and multi-Cox regression analyses.

Additional file 5: Table S5. GSEA results showing the top ten enriched KEGG and GO terms in the high-risk patient group.

Additional file 6: Table S6. Infiltrated immune cells in the TME were associated with the high-risk group on different platforms.

Additional file 7: Fig. S1. Correlations between lncRNA expression and clinicopathological characteristics, such as age and gender, in CRC.

Additional file 8: Fig. S2. The 16 immunotherapeutic anticancer drugs that showed lower IC50 values in the high-risk group.

Additional file 9: Fig. S3. The 22 chemotherapeutic or targeted drugs that showed lower IC50 values in the high-risk group.

Additional file 10: Fig. S4. The Uni-Cox and Multi-Cox regression analyses to estimate the multiple clinical factors and the rickscore for OS and the 8 lncRNA expression with the OS, respectively in the clincal-CRC cohort.

Acknowledgements

We thank the reviewers for their constructive comments. We thank the Cancer Research Center and the Central Laboratory of the First Affiliated Hospital of Fujian Medical University for providing the research and experimental platform.

Authors' contributions

SC and YX are the designers of this study. CZ analyzes and writes the manuscript. LY and CZ analyzed the data and completed the RT-PCR experiment. CZ and LS download data and statistical analysis. All authors read and approved the final

manuscript.

Funding

This work was supported by the Joint Funds for the Innovation of Science and Technology, Fujian Province [No.2019Y9133] and Fujian Province Finance Project (No.BPB-CSQ2021) of China.

Availability of data and materials

We declared that the data and materials in this study are provided free of charge to scientists for non-commercial purposes.

Declarations

Ethics approval and consent to participate

The study was approved by the Ethics Committee of First Affiliated Hospital of Fujian Medical University. All patients have signed an informed consent form.

Consent for publication

All authors Consent for publication.

Competing interests

The authors declared that they have no conficts of interest to this work.

References

[1] Siegel Rebecca L, Miller Kimberly D, Fuchs Hannah E, et al. Cancer Statistics, 2021[J]. CA Cancer J Clin, 2021, 71: 7-33.

[2] Sung Hyuna, Ferlay Jacques, Siegel Rebecca L, et al. Global Cancer Statistics 2020: GLOBOCAN Estimates of Incidence and Mortality Worldwide for 36 Cancers in 185 Countries[J]. CA Cancer J Clin, 2021, 71: 209-249.

[3] Agarwal Parul, Le Dung T, Boland Patrick M, Immunotherapy in colorectal cancer[J]. Adv Cancer Res, 2021, 151: 137-196.

[4] Feng Mei, Zhao Zhongwei, Yang Mengxuan, et al. T-cell-based immunotherapy in colorectal cancer[J]. Cancer Lett, 2021, 498: 201-209.

[5] Um Wooram, Ko Hyewon, You Dong Gil, et al. Necroptosis-Inducible Polymeric Nanobubbles for Enhanced Cancer Sonoimmunotherapy[J]. Adv Mater, 2020, 32: e1907953.

[6] Zhang Duan-Wu, Shao Jing, Lin Juan, et al. RIP3, an energy metabolism regulator that switches TNF-induced cell death from apoptosis to necrosis[J]. Science, 2009, 325: 332-6.

[7] Aaes Tania Love, Kaczmarek Agnieszka, Delvaeye Tinneke, et al. Vaccination with Necroptotic Cancer Cells Induces Efficient Anti-tumor Immunity[J]. Cell Rep, 2016, 15: 274-87.
[8] Lomphithak Thanpisit, Akara-Amornthum Perawatt, Murakami Keigo, et al. Tumor necroptosis is correlated with a favorable immune cell signature and programmed death-ligand 1 expression in cholangiocarcinoma[J]. Sci Rep, 2021, 11: 11743.
[9] Seneviratne Danushka, Ma Jihong, Tan Xinping, et al. Genomic instability causes HGF gene activation in colon cancer cells, promoting their resistance to necroptosis[J]. Gastroenterology, 2015, 148: 181-191.e17.
[10] Han Qinrui, Ma Ye, Wang Hao, et al. Resibufogenin suppresses colorectal cancer growth and metastasis through RIP3-mediated necroptosis[J]. J Transl Med, 2018, 16: 201.
[11] Chen Sian, Shen Xian. Long noncoding RNAs: functions and mechanisms in colon cancer[J]. Mol Cancer, 2020, 19: 167.
[12] Jiang Na, Zhang Xiaoyu, Gu Xuejun, et al. Progress in understanding the role of lncRNA in programmed cell death[J]. Cell Death Discov, 2021, 7: 30.
[13] Wang K, Liu F, Liu C-Y, et al. The long noncoding RNA NRF regulates programmed necrosis and myocardial injury during ischemia and reperfusion by targeting miR-873[J]. Cell Death Differ, 2016, 23: 1394-405.
[14] Zhao Zirui, Liu Haohan, Zhou Xingyu, et al. Necroptosis-Related lncRNAs: Predicting Prognosis and the Distinction between the Cold and Hot Tumors in Gastric Cancer[J]. J Oncol, 2021, 2021: 6718443.
[15] Geeleher Paul, Cox Nancy J, Huang R Stephanie. Clinical drug response can be predicted using baseline gene expression levels and in vitro drug sensitivity in cell lines[J]. Genome Biol, 2014, 15: R47.
[16] Qin Fengxia, Xu Houxi, Wei Guoli, et al. A Prognostic Model Based on the Immune-Related lncRNAs in Colorectal Cancer[J]. Front Genet, 2021, 12: 658736.
[17] Zhao Zhan, Yang Ya-Bing, Li Xin-Yuan, et al. Comprehensive Analysis of N6-Methyladenosine-Related lncRNA Signature for Predicting Prognosis and Immune Cell Infiltration in Patients with Colorectal Cancer[J]. Dis Markers, 2021, 2021: 8686307.
[18] Xu Guoqiang, Yang Mei, Wang Qiaoli, et al. A Novel Prognostic Prediction Model for Colorectal Cancer Based on Nine Autophagy-Related Long Noncoding RNAs[J]. Front Oncol, 2021, 11: 613949.
[19] Peng Yurui, Xu Chenxin, Wen Jun, et al. Fatty Acid Metabolism-Related lncRNAs Are Potential Biomarkers for Predicting the Overall Survival of Patients With Colorectal Cancer[J]. Front Oncol, 2021, 11: 704038.
[20] Liu Chuan, Hu Chuan, Li Jianyi, et al. Identification of Epithelial-Mesenchymal Transition-Related lncRNAs that Associated With the Prognosis and Immune Microenvironment in Colorectal Cancer[J]. Front Mol Biosci, 2021, 8: 633951.
[21] Ding Chengsheng, Shan Zezhi, Li Mengcheng, et al. Exploration of the Associations of lncRNA Expression Patterns with Tumor Mutation Burden and Prognosis in Colon Cancer[J]. Onco Targets Ther, 2021, 14: 2893-2909.
[22] Bennett Ira M, Farfano Hebe M Vanegas, Bogani Federica, et al. Active transport of Ca2+ by an artificial photosynthetic membrane[J]. Nature, 2002, 420: 398-401.
[23] Wang Chenfei, Lu Yunying, Chen Li, et al. Th9 cells are subjected to PD-1/PD-L1-mediated inhibition and are capable of promoting CD8 T cell expansion through IL-9R in colorectal

cancer[J]. Int Immunopharmacol, 2020, 78: 106019.
[24] Choi Yong Won, Kim Young Hwa, Oh Seung Yeop, et al. Senescent Tumor Cells Build a Cytokine Shield in Colorectal Cancer[J]. Adv Sci (Weinh), 2021, 8: 2002497.
[25] Jary Marine, Liu Wen-Wei, Yan Dongyao, et al. The immune microenvironment in patients with mismatch-repair-proficient oligometastatic colorectal cancer exposed to chemotherapy: the randomized MIROX GERCOR cohort study[J]. Mol Oncol, 2021, 11,25. doi: 10.1002/1878-0261.13173. PMID: 34954864.
[26] Ding Sisi, Lv Xinlu, Liu Zhiju, et al. Overexpression of B7-H4 is associated with infiltrating immune cells and poor prognosis in metastatic colorectal cancer[J]. Int Immunopharmacol, 2021, 90: 107144.
[27] Nestarenkaite Ausrine, Fadhil Wakkas, Rasmusson Allan, et al. Immuno-Interface Score to Predict Outcome in Colorectal Cancer Independent of Microsatellite Instability Status[J]. Cancers (Basel), 2020, 12(10):2902.
[28] Yilin Lin, Xiaoxian Pan, Zhihua Chen, et al. Prognostic value and immune infiltration of novel signatures in colon cancer microenvironment[J]. Cancer Cell Int,2021, 21(1):679.
[29] Wang Ning, Liu Dingsheng. Identification and Validation a Necroptosis-related Prognostic Signature and Associated Regulatory Axis in Stomach Adenocarcinoma[J]. Onco Targets Ther, 2021,14:5373-5383.
[30] Bolik Julia, Krause Freia, Stevanovic Marija, et al. Inhibition of ADAM17 impairs endothelial cell necroptosis and blocks metastasis[J]. J Exp Med, 2022, 219(1):e20201039.
[31] Yan Jiong, Wan Peixing, Choksi Swati, et al. Necroptosis and tumor progression [J]. Trends Cancer, 2021, 8(1):21-27.
[32] Han Qinrui, Ma Ye, Wang Hao, et al. Resibufogenin suppresses colorectal cancer growth and metastasis through RIP3-mediated necroptosis[J]. J Transl Med, 2018, 16: 201.
[33] Strilic Boris, Yang Lida, Albarrán-Juárez Julián, et al. Tumour-cell-induced endothelial cell necroptosis via death receptor 6 promotes metastasis[J]. Nature, 2016, 536: 215-8.
[34] Sprooten Jenny, De Wijngaert Pieter, Vanmeerbeerk Isaure, et al. Necroptosis in Immuno-Oncology and Cancer Immunotherapy[J]. Cells, 2020, 9(8): 1823.
[35] Galon Jérôme, Bruni Daniela. Approaches to treat immune hot, altered and cold tumours with combination immunotherapies[J]. Nat Rev Drug Discov, 2019, 18: 197-218.
[36] Zhang Chong, Wang Xiang-Yu, Zhang Peng, et al. Cancer-derived exosomal HSPC111 promotes colorectal cancer liver metastasis by reprogramming lipid metabolism in cancer-associated fibroblasts[J]. Cell Death Dis, 2022, 13: 57.
[37] Zhang Chao, Zhou Chang, Wu Xiao-Jin, et al. Human CD133-positive hematopoietic progenitor cells initiate growth and metastasis of colorectal cancer cells[J]. Carcinogenesis, 2014, 35: 2771-7.
[38] Yang Chaogang, Dou Rongzhang, Wei Chen, et al. Tumor-derived exosomal microRNA-106b-5p activates EMT-cancer cell and M2-subtype TAM interaction to facilitate CRC metastasis[J]. Mol Ther, 2021, 29: 2088-2107.
[39] Wu Xuehui, Lan Xiaoliang, Hu Wanming, et al. CMTM6 expression in M2 macrophages is a potential predictor of PD-1/PD-L1 inhibitor response in colorectal cancer[J]. Cancer Immunol Immunother, 2021, 70(11):3235-3248.
[40] Lalos Alexandros, Tülek Ali, Tosti Nadia, et al. Prognostic significance of CD8+ T-cells density in stage III colorectal cancer depends on SDF-1 expression[J]. Sci Rep, 2021, 11: 775.

[41] Lam Jian Hang, Hong Michelle, Koo Si-Lin, et al. CD30OX40 Treg is associated with improved overall survival in colorectal cancer[J]. Cancer Immunol Immunother, 2021, 70: 2353-2365.
[42] Hardman Clayton, Ho Stephen, Shimizu Akira, et al. Synthesis and evaluation of designed PKC modulators for enhanced cancer immunotherapy[J]. Nat Commun, 2020, 11: 1879.
[43] Chen Mei-Hua, Wang Yu-Hui, Sun Bing-Jing, et al. HIF-1αactivator DMOG inhibits alveolar bone resorption in murine periodontitis by regulating macrophage polarization [J]. Int Immunopharmacol, 2021, 99: 107901.
[44] Wang Huafeng, Zhang Huan, Wang Yanxia, et al. Embelin can protect mice from thioacetamide-induced acute liver injury[J]. Biomed Pharmacother, 2019, 118: 109360.
[45] Mousset Charlotte M, Hobo Willemijn,,Ji Yun, et al. Ex vivo AKT-inhibition facilitates generation of polyfunctional stem cell memory-like CD8 T cells for adoptive immunotherapy[J]. Oncoimmunology, 2018, 7: e1488565.
[46] Chen Jingyi, Song Yuxuan, Li Mei, et al. Comprehensive analysis of ceRNA networks reveals prognostic lncRNAs related to immune infiltration in colorectal cancer[J]. BMC Cancer, 2021, 21: 255.
[47] Dong Xinhua, Yang Zhen, Yang Hongwei, et al. Long Non-coding RNA MIR4435-2HG Promotes Colorectal Cancer Proliferation and Metastasis Through miR-206/YAP1 Axis [J]. Front Oncol, 2020, 10: 160.
[48] Aguilera Todd A, Rafat Marjan, Castellini Laura, et al. Reprogramming the immunological microenvironment through radiation and targeting Axl[J]. Nat Commun, 2016, 7: 13898.
[49] Noman Muhammad Zaeem, Berchem Guy, Janji Bassam. Targeting autophagy blocks melanoma growth by bringing natural killer cells to the tumor battlefield[J]. Autophagy, 2018, 14: 730-732.
[50] Guisier Florian, Dubos-Arvis Catherine, Viñas Florent, et al. Efficacy and Safety of Anti-PD-1 Immunotherapy in Patients With Advanced NSCLC With BRAF, HER2, or MET Mutations or RET Translocation: GFPC 01-2018[J]. J Thorac Oncol, 2020, 15: 628-636.
[51] Zhang Shujun, Li Juan, Gao Huiru, et al. lncRNA Profiles Enable Prognosis Prediction and Subtyping for Esophageal Squamous Cell Carcinoma[J]. Front Cell Dev Biol, 2021, 9: 656554.

Supplementary Files

This is a list of supplementary files associated with this preprint. Click to download.

- Additionalfile1SupplementTable1.docx
- Additionalfile2SupplementTable2.doc
- Additionalfile3SupplementTable3.doc
- Additionalfile4SupplementTable4.doc
- Additionalfile5SupplementTable5.doc
- Additionalfile6SupplementTable6..doc
- Additionalfilethefigures.doc